

# Rossby wave propagation into the tropics in two GFDL general circulation models

George N Kiladis, Steven B Feldstein

Cooperative Institute for Research in Environmental Sciences, University of Colorado, Boulder, CO 80309, USA

Received: 30 October 1992/Accepted: 5 July 1993

**Abstract.** During the northern winter the eastern Pacific is characterized by upper level westerly flow extending from the equator into the midlatitudes of both hemispheres. Theoretical and simple modeling studies suggest that such a region should favor the penetration of Rossby waves into the tropics from higher latitudes. Observational results by Kiladis and Weickmann using 200 mb data indicate that Rossby waves do indeed propagate freely into the tropical eastern Pacific during the northern winter from the Asian jet exit region. They also confirmed that cross-equatorial dispersion of energy from the Northern into the Southern Hemisphere occurs frequently. The present study examines these interactions in climatological runs of two GFDL GCMs. The northern wintertime mean states of these models are characterized by a rather realistically simulated upper level westerly regime in the tropical Pacific. Despite the relative weakness of the Asian jet and wave activity with respect to observations, propagation of Rossby waves into the tropics is present in both models, and these waves are strongly positively tilted as seen in the observations. A momentum budget of the zonal wind and E vector diagnostics over the tropical Pacific indicate that these transients are an important component of the momentum balance of the equatorial westerlies in both the observations and in the models.

## Introduction

The interaction between the tropics and extratropics is of central importance in the study of the general circulation of the atmosphere. Much of the early work on this topic focused on the effect of the “critical level”,

where the zonal wind speed equals the zonal wave phase speed (e.g., Charney 1969; Bennett and Young 1971; Webster 1973; Warn and Warn 1978). These studies suggested that the critical level should act as a barrier to the equatorward propagation of wave energy, while further simple dynamical modeling studies suggested that substantial Rossby wave interaction between the tropics and extratropics should be restricted to regions of westerly flow extending from the midlatitudes well into the tropics (Webster and Holton 1982; Branstator 1983; Karoly 1983; Zhang and Webster 1992).

There have been several observational studies citing evidence of equatorward propagation of wave energy in the eastern Pacific (e.g., Blackmon et al. 1984a,b; Liebmann and Hartmann 1984; Hsu and Lin 1992). In two recent papers, Kiladis and Weickmann (1992a,b, hereafter referred to as KW) showed that the region of low latitude upper tropospheric westerly flow over the central and eastern Pacific and Atlantic sectors during the northern winter is indeed characterized by frequent wave activity propagation from the extratropics into low latitudes. These waves were shown to be strongly tied to tropical convection within the ITCZ north of the equator in the eastern Pacific, such that troughs appear to trigger the convection on times scales ranging from one to two weeks. These convective outbreaks are associated with a signal of poleward propagating “cloud bands” frequently seen on satellite photos. The existence of these interactions is strongly dependent on the occurrence of low latitude westerly flow, such that the waves appear to be much less frequent in the region of upper level equatorial easterly flow in the Eastern Hemisphere.

It is natural to ask whether the low latitude Rossby wave activity seen in observations exists in GCMs as well. It seems reasonable to expect the existence of such wave activity at low latitudes in GCMs, since the upper level time mean flow in most of these models includes a region of westerlies from pole to pole in the eastern Pacific and Atlantic sectors during the northern winter. In this study we will examine the propaga-

---

This paper was presented at the Second International Conference on Modelling of Global Climate Variability, held in Hamburg 7–11 September 1992 under the auspices of the Max Planck Institute for Meteorology. Guest Editor for these papers is L. Dümenil

tion of waves from the midlatitudes into the tropics in two GFDL GCMs with different resolutions. We will also investigate whether these waves have a substantial impact on the mean state of the model tropical Pacific. The model wave activity will be compared with that from National Meteorological Center (NMC) observational data, as was used in KW. In the next section we describe the data, models, and methodology used for this study. The results are then shown, followed by a discussion and conclusions.

## Data and methodology

### Data

Two GFDL GCMs are utilized for this study, and diagnostics from these models are compared with observational results from NMC data. As in KW, the observational data set consists of 12 years of 200 mb  $u$  and  $v$  components from 1979 through 1990. These data have been shown by KW to be adequate over the tropical Pacific for the present applications.

The GFDL models are of two resolutions, R15 and R30. An early version of the R30 model is used here, while the R15 version is the same model which has been used in a variety of climate studies (e.g., Lau 1985; Lau and Lau 1986). This model has been described in some detail by Manabe and Hahn (1981) and Lau (1981). The dynamics of the R30 version are similar, although with twice the horizontal resolution. Both models have nine vertical sigma levels, realistic orography, and predicted clouds, with the R30 version employing a gravity wave drag parameterization.

We utilize a 10 year sample of climate runs from each model, with insolation, sea surface temperature, and sea ice varying through the same seasonal cycle during each model year. The GCM data are logarithmically interpolated from sigma surfaces to the 205 mb pressure surface. The 205 mb model time mean zonal winds (refer to Fig. 4) are reasonable within the Pacific basin, although the Asian jet is too weak and its exit region is somewhat too far west compared with observations. The equatorial zero zonal wind line is close to observations in the R15, and 30° longitude too far west in the R30. Nevertheless, westerly flow extending from midlatitudes of both hemispheres to the equator is present in both models, and is quite realistically simulated, especially in the R15 version.

### Filtering

As shown in KW, the wave activity in the tropics in the NMC analyses can be isolated quite easily through cross-correlation techniques. Prior to performing the cross-correlations, it is necessary to first subtract out the seasonal cycle and filter the data to remove variability from frequency bands unrelated to fluctuations of interest. In KW, it was found that the observed wintertime wave activity associated with tropical convec-

tion over the eastern Pacific was most pronounced in the 6–14 day band pass filtered data. The six day cutoff was utilized to filter out synoptic scale baroclinic transient fluctuations, which were shown to add considerable noise to the cross correlation results. The 14 day cutoff was based on frequency spectra of outgoing longwave radiation (OLR) and 200 mb relative vorticity, which showed a tendency for spectral peaks in the 8 to 12 day range over the tropical eastern Pacific.

In both models, the power spectra of relative vorticity (not shown) are less red than in observations of the equatorial east Pacific. However, there is in general more power at 8 to 10 days in the model vorticity than other frequencies when compared to a red noise spectrum determined from the lag one autocorrelation. Later it is shown that Rossby wave activity is readily detected in the 6–14 day band in the GCMs, so we retain this band for model cross-correlations as well. As in observations, cross-correlations which include higher frequencies (e.g., 2–14 day filtered data) yield similar but noisier results than those using 6–14 day data.

Other diagnostics such as the zonal momentum budget and the two dimensional E vector ( $\overline{v'^2 - u'^2}$ ,  $-\overline{u'v'}$ ) of Hoskins et al. (1983) have been calculated for both the models and the observations over the Pacific sector. In order to simplify the E vector calculations, perturbations were low and high pass instead of band pass filtered with a 14 day cutoff. A Lanczos digital filter was used for this purpose (Duchon 1979). Second moment quantities were obtained by first filtering the data and then calculating the products, as has been done in numerous other studies (e.g., Hoskins et al. 1983).

## Results

### Cross-correlations

It was found that the wave activity of interest could be readily identified through the cross-correlation of vorticity at a base point in the tropical eastern Pacific and the wind at all other points on the globe. Following the technique used in KW, filtered 6–14 day relative vorticity at 200 mb at a base point was regressed separately against the identically filtered  $u$  and  $v$  components at all other grid points in both the observations and the models. These regressions were used to reconstruct the global wind anomaly pattern associated with an arbitrary anomaly in 6–14 day relative vorticity at the base point. The correlation coefficient between the base vorticity and the wind components also gives a measure of the strength of the linear relationship at each grid point. Lagged correlations and regressions were also calculated for several days before and after the contemporaneous cross-correlation (see KW for a more detailed discussion of this technique).

The best results in the NMC data were obtained with relative vorticity at about 10° N in the 160° W–120° W longitude range, in the region of strongest equatorial westerlies at upper levels. Figure 1 shows

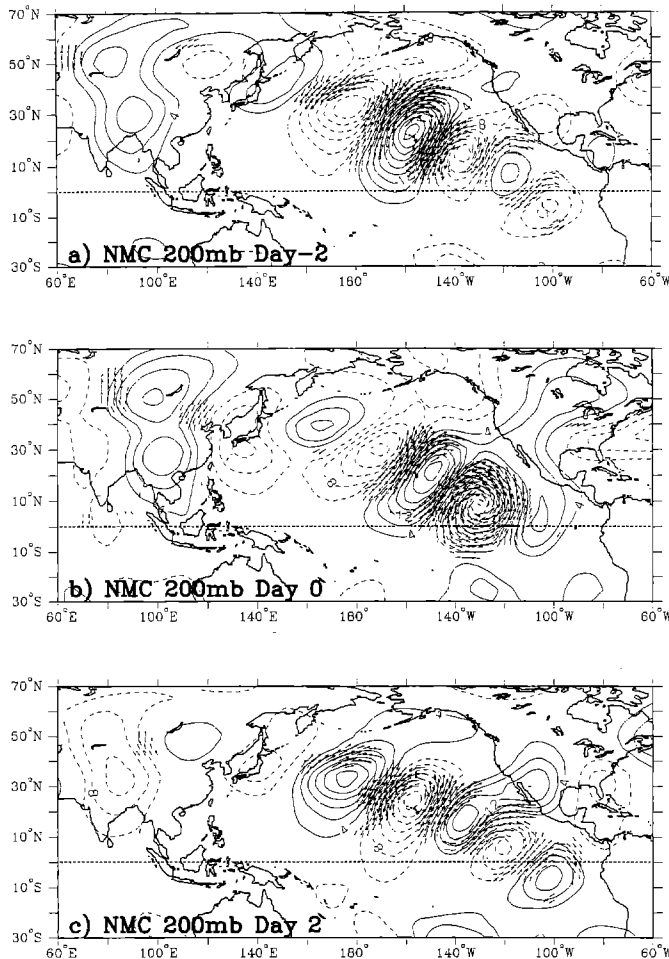


**Fig. 1a-c.** Observed NMC 200 mb streamfunction and locally significant wind perturbations in the 6–14 day band associated with a vorticity anomaly of  $12.3 \times 10^{-6} \text{ s}^{-1}$  (+1 standard deviation) at  $10^\circ \text{ N}$ ,  $160^\circ \text{ W}$ , during December–February 1979–90. The contour interval is  $4 \times 10^5 \text{ m}^2 \text{ s}^{-1}$  with negative contours *dashed* and the zero contour omitted. The largest wind vectors are about  $5 \text{ m s}^{-1}$ . **a** Two days prior to the maximum vorticity anomaly at the base point (day-2); **b** simultaneous relationship (day 0); **c** day +2

the results for relative vorticity at  $10^\circ \text{ N}$ ,  $130^\circ \text{ W}$  during December–February 1979–90. Regressed  $u$  and  $v$  anomalies are computed for a +1 standard deviation in vorticity at the base point ( $12.3 \times 10^{-6} \text{ s}^{-1}$ ). The associated streamfunction perturbation along with the statistically significant wind vector anomalies are plotted for the lag 0 correlation in Fig. 1b. Statistical significance is calculated locally using a standard t-test, with a perturbation wind vector plotted if either the  $u$  or  $v$  component is significantly correlated with vorticity at the base point. In order to provide a smooth picture of the circulation, the streamfunction anomaly is plotted everywhere regardless of its statistical significance.

The contemporaneous (day 0) cross-correlation shows that a positive vorticity perturbation just north of the equator in the eastern Pacific is associated with a wave train to its northwest. These waves are positively tilted, and thus are directing wave energy equatorward and transporting westerly momentum poleward. The

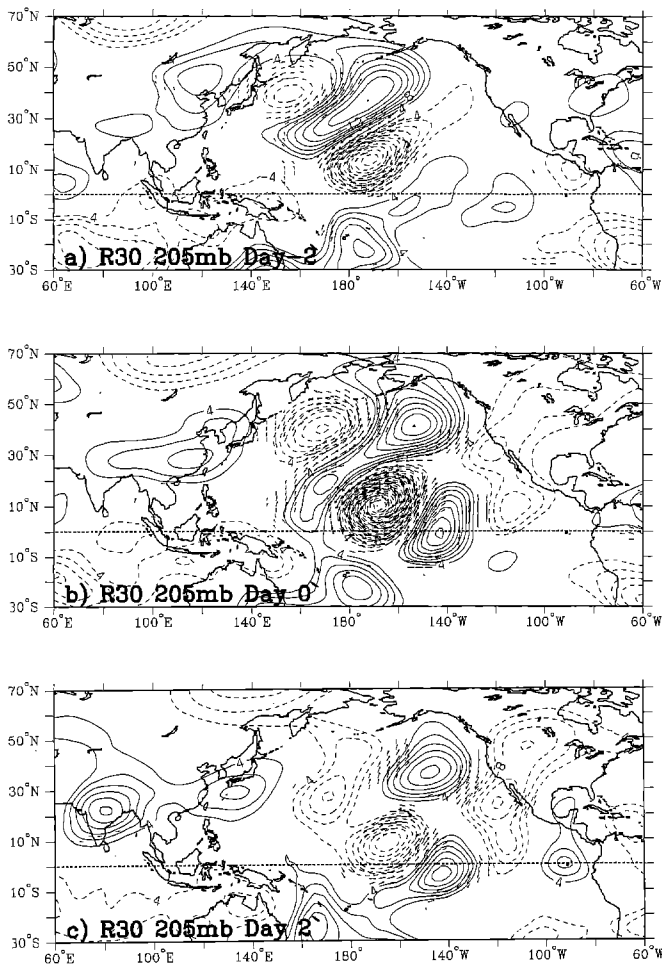
highest amplitude features, along with most of the statistically significant vectors are located in the region of the base point, which is to be expected with data that is so strongly spatially autocorrelated.

Figure 1a and 1c shows the results of lagged cross-correlations between circulation two days prior to (day-2) and two days following (day+2) the maximum vorticity anomaly at the basepoint. By tracking the vorticity centers through the period one can see that the individual waves are indeed propagating equatorward from the region of the Asian jet near Japan. It is likewise apparent that wave energy is dispersing equatorward, since circulation centers strengthen successively downstream at the expense of those upstream, so that the group speed exceeds the phase speed of the waves. Also evident is that the wave energy disperses across the equator into the Southern Hemisphere, with the development of a circulation centered at  $10^\circ \text{ S}$ ,  $100^\circ \text{ W}$ .

The question of the statistical significance of the spatial patterns of filtered data, called field significance (e.g., Livezey and Chen 1983), is discussed in more detail in KW. Here we simply point out that the cross-correlation results are very robust, both to changes in the location of the base point (the entire pattern shifts westward or eastward with a corresponding shift in the base point) and to a choice of independent periods used to construct the regressed perturbations (two independent samples yield nearly identical results).

Figure 2 shows the results of an identical calculation for relative vorticity at  $10^\circ \text{ N}$ ,  $170^\circ \text{ E}$  in the R30 GCM. Results are similar for the R15 GCM and will not be shown. In these calculations, unlike in the NMC data, two separate wave trains are evident. One wave train propagates directly eastward from the Asian jet exit region toward North America. The other wave train propagates equatorward and disperses downstream to cross the equator into the Southern Hemisphere. The individual disturbances that comprise both wave trains are positively tilted, and the horizontal movement of the largest amplitude streamfunction centers in both wave trains indicates a southeastward component of the group velocity.

In addition, the equatorial circulations between  $120^\circ \text{ W}$ – $80^\circ \text{ W}$  in Fig. 2 have characteristics of mixed Rossby-gravity waves. Longer time sequences of these maps show that these waves move westward along the equator and have an eastward group velocity. Little evidence for these waves was found in the NMC data, yet the presence of equatorially trapped Rossby-gravity waves is evident in the observational study of Liebmann and Hendon (1990) and Hendon and Liebmann (1991), with these disturbances being located farther west and most pronounced during boreal fall. Likewise, Randel (1992) found Rossby-gravity wave activity in ECMWF data of the upper troposphere over the eastern equatorial Pacific. Again these waves were most pronounced in the late summer-early fall, and appeared to be generated by extratropical forcing. The same process was also observed in a shallow water model by Zhang and Webster (1992). Since these



**Fig. 2a-c.** As in Fig. 1, except for the R30 GCM and vorticity at  $10^{\circ}\text{N}$ ,  $170^{\circ}\text{W}$ . In this case the standard deviation of vorticity is  $11.1 \times 10^{-6} \text{ s}^{-1}$

waves are not evident in the NMC data for December–February, they will not be discussed further.

The zonal phase speed of the transient eddies in the eastern tropical Pacific is calculated from the lagged cross-correlations in Figs. 1 and 2. This calculation is performed by determining how far the centers of the high and low streamfunction move in the zonal direction between successive lags. It was found that the zonal phase speed is approximately  $3 \text{ ms}^{-1}$  in the NMC data and about  $2 \text{ ms}^{-1}$  in the R30 GCM. The critical lines for these transient eddies, i.e., where the climatological zonal wind equals the phase speed of the transient eddies, should be quite close to the zero zonal wind line in Fig. 4a,b since the phase speed of the eddies is itself nearly zero. We can clearly see from Figs. 1 and 2 that the transient eddies are bounded by their critical lines in both the observational data and the GCM, as there is little wave activity in the region of negative zonal wind. This is consistent with the observational study of Randel and Held (1991), who used zonally average ECMWF data to show that synoptic-scale transient eddies in the extratropics are also bounded by their critical lines.

While the waves in the models are not as coherent or as statistically significant as those in the observations, particularly following the peak in vorticity (day+2), they have similar amplitude. For example, the 6–14 day filtered standard deviation of relative vorticity is  $11.1 \times 10^{-6} \text{ s}^{-1}$  and  $12.0 \times 10^{-6} \text{ s}^{-1}$  for the R30 and R15 models, respectively, in those regions where the waves have maximum amplitude in the models (near the dateline). However, a notable difference is that the model waves are best developed in a narrower region ( $170^{\circ}\text{E}$ – $140^{\circ}\text{W}$ ), farther to the west than in observations where the waves peak in the region  $170^{\circ}\text{W}$ – $110^{\circ}\text{W}$ . Outside of this region the waves are present, but have significantly lower amplitude.

In KW, the waves were initially isolated through cross correlations between OLR and 200 mb circulation, such that the waves appeared to trigger convection in the ITCZ. Cross-correlations between precipitation and 200 mb circulation in both models revealed no discernible relationship. This is perhaps related to deficiencies in the convective parameterization, as well as the resolution of the models, which is not high enough to accurately simulate such a narrow convergence zone as is found during the northern winter in the eastern Pacific.

### Momentum budget

The positively tilted waves identified in the previous section transport westerly momentum poleward out of the tropics, and should thus serve to weaken the westerly flow at low latitudes. In order to assess whether the eddies play an important role in the climatology of the eastern tropical Pacific during winter, the zonal momentum budget is examined. The observational budget is obtained from five years of January NMC data from 1987–91. The calculations for the R30 and R15 models utilize ten years of model January data.

For this analysis, the zonal wind tendency equation is written in the following form:

$$\frac{\partial \bar{u}}{\partial t} = -\bar{u} \frac{\partial \bar{u}}{\partial x} - \bar{v} \frac{\partial \bar{u}}{\partial y} + \overline{fv_{ag}} - \frac{\partial(\overline{u'u'})}{\partial x} - \frac{\partial(\overline{u'v'})}{\partial y} = R, \quad (1)$$

where the overbar denotes the time mean and the prime a deviation from the time mean. In (1),  $u$  and  $v$  denote the zonal and meridional winds, respectively,  $v_{ag}$  is the ageostrophic meridional wind,  $f$  the Coriolis parameter, and  $R$  a residual. Note that we do not explicitly calculate the vertical advection of the zonal wind, so it is included in the residual. In the NMC data over the eastern tropical Pacific,  $R$  is between five and ten times smaller than every other term in (1). Therefore, this approximate form of the budget equation is sufficient for determining whether transient eddies strongly contribute to the momentum budget of the zonal wind in the region of interest.

The ageostrophic Coriolis acceleration (term  $A$ ) and the total (unfiltered) transient eddy momentum

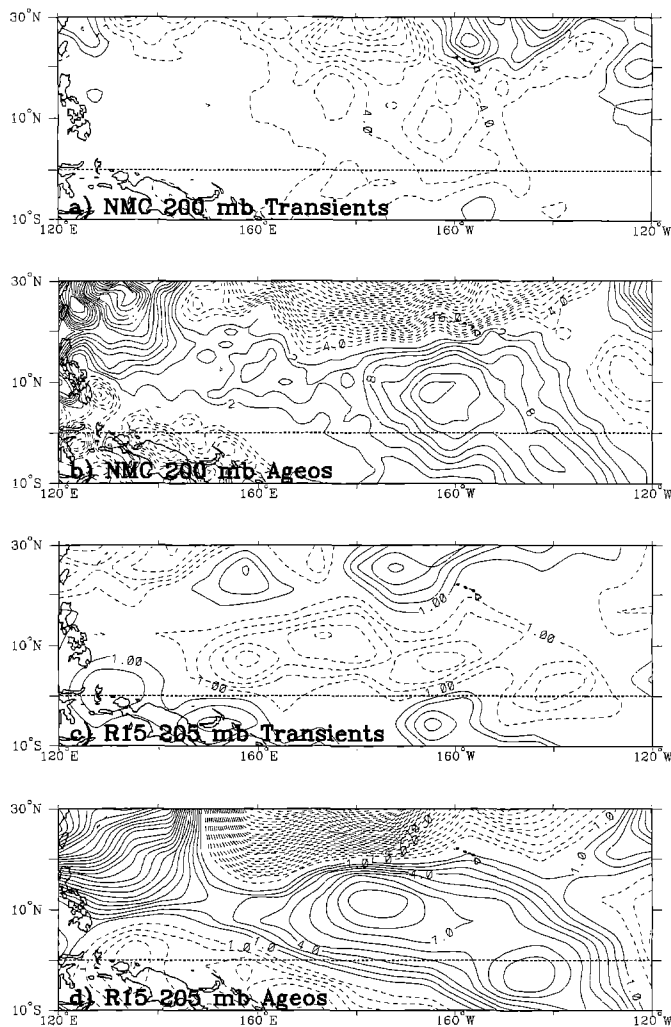


**Fig. 3a-d.** Transient eddy momentum flux convergence (Term B in equation 1) for **a** 200 mb January 1987–91 NMC data and **c** 10 years of 205 mb January R15 data. Ageostrophic acceleration term ( $f'v_{ag}$ ) for **b** 200 mb January 1987–91 NMC data; **d** 10 years of 205 mb January R15 data. The contour interval is  $2 \times 10^{-5} \text{ ms}^{-2}$  in **a** and **b** and  $1 \times 10^{-5} \text{ ms}^{-2}$  in **c** and **d**. Negative contours are dashed, and the zero contour has been omitted

flux convergence (the two terms that comprise  $B$ ) are shown in Fig. 3a,b for the NMC data. It can be seen that throughout most of the eastern tropical Pacific the eddy momentum flux convergence is opposite in sign and has a magnitude about two thirds that of the ageostrophic Coriolis acceleration. Therefore, the transient eddies oppose the tendency for the Coriolis torque to accelerate the zonal wind in this region. Such behavior resembles that observed for the zonally-averaged flow (see Palmen and Newton 1969, pp 19–20) and in idealized barotropic models (Held and Phillips 1987, 1990).

Similar calculations were performed for 6–14 day band pass data, as well as low and high pass transients with a 14 day cutoff (not shown). The filtered budgets were calculated by replacing the total  $u'$  and  $v'$  in Eq. (1) by their filtered perturbations. These results show that the 6–14 day transient fluxes have a similar pattern

to the high pass and total transients and contribute to a substantial fraction (approaching 50%) of the momentum budget in the subtropical Pacific. In contrast, budget terms involving the interaction between low, band, and high pass eddies were found to be negligible in the subtropics. Thus, the 6–14 day transients identified in the previous section are crucial to the maintenance of the upper level zonal wind budget in the tropical eastern Pacific.

Since the results from the R15 and R30 models were found to be similar, only those from the R15 model are presented. As with the NMC data, for both models, the residual term was also found to be much smaller than the remaining terms in (1). Band pass and high pass fluctuations were again found to contribute a large fraction of the transient forcing in these budgets, with interactions between these and low pass eddies negligible. The ageostrophic Coriolis acceleration and the total transient eddy momentum flux convergence are shown for the R15 model in Fig. 3c,d. There are marked similarities between the R15 GCM and the NMC data both in horizontal structure and in sign, although the magnitude of both of the model terms is only about one half that in the NMC data, and the contour intervals have been adjusted accordingly. Thus, in the GCM, the transient eddies also play an important role in the zonal wind climatology of the eastern tropical Pacific. Differences between the model and observations will be discussed in more detail next.

#### *E* vectors

Figure 4 shows the two dimensional  $E$  vector fields for January at 200 mb for transient fluctuations less than 14 days in the observations and models. The  $E$  vector gives information on the anisotropy and group velocity of the transients, and its divergence is related to the forcing of the mean flow by the transients. Since we are interested in the occurrence of positively tilted waves propagating into the tropics, we search for regions with southeastward or southwestward pointing vectors at low latitudes. This would signify anisotropic transient eddies (a substantially positive or negative  $x$  component,  $v'^2 - u'^2$ ), with northward directed momentum fluxes and thus southward energy dispersion (a negative  $y$  component,  $-u'v'$ ). In observations (Fig. 4a) an extensive region of such vectors exists from the Asian jet exit region into the tropical eastern Pacific (see also Wallace and Lau 1985 and Hoskins et al. 1983). These  $E$  vectors are for the most part pointing southeastward, indicative of the type of eddy activity described in the previous section. There is convergence of the vectors in the vicinity of the ITCZ at about  $10^\circ \text{ N}$ , which is strongest from  $160^\circ \text{ W}$  to about  $130^\circ \text{ W}$ , or precisely in the region of maximum cross correlation of the vorticity with the wind field in the NMC data.

As shown in Hoskins et al. (1983), the convergence of the  $E$  vectors implies that the eddies are decelerating the local zonal wind. Thus, the picture that emerges is that the transient activity acts as a brake on the mean

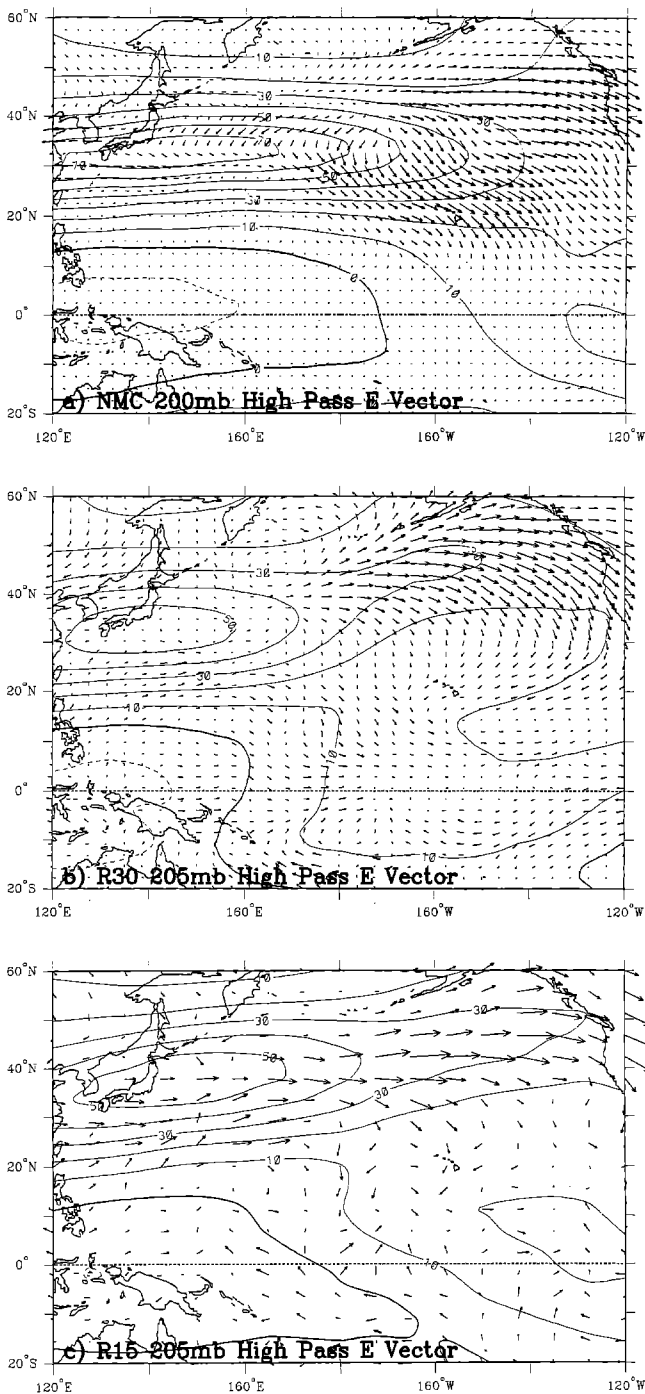


**Fig. 4a-c.** January mean 200 mb E vectors for fluctuations less than 14 days. **a** 1987–91 NMC data; **b** 10 years of January R30 data; **c** 10 years of January R15 data. Contours represent the mean zonal wind, with negative contours *dashed* and a contour interval of  $10 \text{ m s}^{-1}$ . The longest vectors are about  $100 \text{ m}^2 \text{ s}^{-2}$  in **a** and **c**, and about  $50 \text{ m}^2 \text{ s}^{-2}$  in **b**

low latitude westerly flow over the tropical Pacific. This is consistent with the results of the previous subsection, as term  $B$  in (1) can be rewritten as  $\nabla \cdot E - \partial(\bar{v}'v')/\partial x$ , where  $\nabla \cdot E$  denotes the divergence of the  $E$  vector. As is seen in Fig. 4a, the  $E$  vectors do converge in the region where term  $B$  is most negative. In addition, a second set of  $E$  vectors is seen pointing

toward North America. These vectors are at a latitude slightly poleward of the Asian jet and have a small southward component. Thus, observations show two regions of wave activity propagation; one eastward toward North America and the other southeastward into the tropical eastern Pacific.

The  $E$  vectors from high frequency transients in the GCMs (Fig. 4b,c) are generally lower in amplitude than those in the observations, and their magnitudes have been rescaled for comparison. These vectors also point toward both North America and the tropical eastern Pacific. However, unlike Fig. 4a, the dominant  $E$  vectors are those that remain poleward of the Asian jet, implying that the amount of eddy energy that reaches the tropical eastern Pacific in the GCM is less than that seen in observations. Notwithstanding this, several of the model's propagation characteristics are rather realistic in this region. In the R30 model, there is a broad region of southeastward pointing vectors from the southern flank of the Asian jet exit region into the tropics from about  $160^\circ \text{ E}$  to  $160^\circ \text{ W}$ . As the jet in the R30 model is shifted westward relative to that in observations, the eddy energy that reaches the tropics is also too far west. On the other hand, the R15 model has a better geographic positioning of both its Asian jet and tropical westerlies when compared with the observations. Also, its  $E$  vectors are more equatorward and have a larger amplitude than those in the R30 model, but these vectors are less coherent and noisier, suggesting erroneous transient-mean flow interaction over the Pacific sector. Nevertheless, on the positive side, the models are obviously capable of producing the type of transient tropical-extratropical interaction seen in observations, which appears to be highly dependent on zonal asymmetries in the base state, even at the relatively low resolution of R15.

#### Discussion and conclusions

Since the models and the observations exhibit differences in their time mean background flow, we expect to see differences in their transient eddy propagation characteristics. In the observations, the latitude of the maximum zonal wind is near  $30^\circ \text{ N}$  at most longitudes throughout the Pacific Ocean. On the other hand, in the central and eastern Pacific Ocean of both GCMs, the latitude of the jet maxima has shifted northward to close to  $45^\circ \text{ N}$ . Through the use of a local application of the quasi-geostrophic refractive index (see Palmer 1982 and Randel and Stanford 1985), we can try to relate this northward shift of the jet to the differences in the wave propagation characteristics between the GCMs and observations.

In analogy to geometric optics, wave activity propagates in the direction of largest refractive index (see Andrews et al. 1987, pp 183–188), which is proportional to the potential vorticity gradient  $\partial Q/\partial y$ . Thus, wave activity should propagate toward a large  $\partial Q/\partial y$ , and in particular, near the latitude of the jet maxima where

$\partial Q/\partial y$  is near its largest value. Since the jets in both models have an erroneous northeastward orientation, one might expect a preference for poleward propagation in the models, and equatorward propagation in observations. Accordingly, the majority of the wave energy that is generated in the Asian jet propagates poleward and eastward and does not reach the tropics. Furthermore, a reduction in the amplitude of the waves that reach the tropics implies a weakening of the eddy driven zonal wind deceleration. This is shown particularly well in Fig. 4b where both the divergence of the E vector is smaller than in observations and the tropical westerlies in the eastern Pacific are stronger than in observations.

In addition to this relationship between the latitude of the Asian jet and the smaller deceleration of the subtropical westerly winds by the transient eddies, the weakness of the Asian jet is another factor that may contribute to the strengthening of the tropical westerlies. This is because the amount of wave energy that is generated via baroclinic energy conversions in the vicinity of the jet should be less than that which is typically observed in the atmosphere. As a result, less wave energy can propagate from the midlatitudes to the tropics and decelerate the zonal wind. Such behavior is consistent with that found by Feldstein and Held (1989) who showed with an idealized quasi-geostrophic model that an increase in the strength of the midlatitude jet results in a greater deceleration of the subtropical zonal winds by the eddies originating in midlatitudes.

As discussed earlier, the Rossby wave activity in the two GCMs is confined to a narrower longitudinal region with respect to observations. Although no explanation is offered for this difference, one must certainly suspect that the differences between the tropical time-mean background flow in the model and in observations accounts for the reduced zonal extent of the eddies in the model.

The results of this study suggest that a more realistic representation of low latitude Rossby waves and tropical-extratropical interaction will result in improved model climatologies. Since much of the Rossby wave energy in the atmosphere is generated in midlatitudes and is dissipated in the tropics, an improved tropical climatology requires a better midlatitude climatology. Furthermore, an inspection of the climatological tropical zonal winds in the R15 model (see Fig. 4c) shows that they more closely resemble the observational mean zonal winds in the tropics than does the R30 model. However, the propagation of the high frequency transient eddies in the R15 model, as represented by E vectors, shows too high an amplitude in the Asian jet and too much noise in the subtropics (compare Fig. 4a and c). This indicates that the R15 model is getting the right low latitude climatology for the wrong reason, since the transients have been improperly modeled.

This study has highlighted some of the strengths and weaknesses of two particular GCMs in modeling the propagation of midlatitude disturbances into the tropics. In particular, the results of this study emphasize

that accurate modeling of these disturbances is expected to improve the climatology of the model tropics. It is hoped that the next generation GCMs with higher vertical and horizontal resolution and new parameterizations will show improvements in these areas.

*Acknowledgements.* We thank Klaus Weickmann for discussions of the momentum budget in the tropics, Mary Jo Nath and Peter Phillips of the Geophysical Fluid Dynamics Laboratory for performing the R15 and R30 GCM experiments, and Sukeyoung Lee for her helpful comments on the first draft of this paper. This work was partially supported by the National Science Foundation under Grant ATM-9012704. Much of the computing for this study was performed at the National Center for Atmospheric Research (NCAR), and we thank the Scientific Computing Division for their help with these calculations (NCAR is supported by the National Science Foundation).

## References

- Andrews DG, Holton JR, Leovy CB (1987) Middle atmospheric dynamics. Academic Press, Orlando Florida, 489 pp
- Bennett JR, Young JA (1971) The influence of latitudinal wind shear upon large-scale wave propagation into the tropics. *Mon Weather Rev* 99:202–214
- Blackmon ML, Lee Y-H, Wallace JM (1984a) Horizontal structure of 500 mb height fluctuations with long, intermediate and short time scales. *J Atmos Sci* 41:961–979
- Blackmon ML, Lee Y-H, Wallace JM, Hsu H-H (1984b) Time variation of 500 mb height fluctuations with long, intermediate and short time scales as deduced from lag-correlation statistics. *J Atmos Sci* 41:981–991
- Branstator G (1983) Horizontal energy propagation in a barotropic atmosphere with meridional and zonal structure. *J Atmos Sci* 40:1689–1708
- Charney JG (1969) A further note on large-scale motions in the tropics. *J Atmos Sci* 26:182–185
- Duchon CE (1979) Lanczos filtering in one and two dimensions. *J Appl Meteorol* 18:1016–1022
- Feldstein SB, Held IM (1989) Barotropic decay of baroclinic waves in a two-layer betaplane model. *J Atmos Sci* 46:3416–3430
- Held IM, Phillips PJ (1987) Linear and nonlinear barotropic decay on the sphere. *J Atmos Sci* 44:200–207
- Held IM, Phillips PJ (1990) A barotropic model of the interaction between the Hadley cell and a Rossby wave. *J Atmos Sci* 47:856–869
- Hendon HH, Liebmann B (1991) The structure and annual variation of antisymmetric fluctuations of tropical convection and their association with Rossby-gravity waves. *J Atmos Sci* 48:2127–2140
- Hoskins BJ, James IN, White GH (1983) The shape, propagation and mean-flow interaction of large-scale weather systems. *J Atmos Sci* 40:1595–1612
- Hsu H-H, Lin S-H (1992) Global teleconnections in the 250-mb streamfunction field during the Northern Hemisphere winter. *Mon Weather Rev* 120:1169–1190
- Karoly DJ (1983) Rossby wave propagation in a barotropic atmosphere. *Dyn Atmos Oceans* 7:111–125
- Kiladis GN, Weickmann KM (1992a) Circulation anomalies associated with tropical convection during northern winter. *Mon Weather Rev* 120:1900–1923
- Kiladis GN, Weickmann KM (1992b) Extratropical forcing of tropical Pacific convection during northern winter. *Mon Weather Rev* 120:1924–1938

- Lau N-C (1981) A diagnostic study of recurrent meteorological anomalies appearing in a 15-year simulation with a GFDL general circulation model. *Mon Weather Rev* 109:2287–2311
- Lau N-C (1985) Modeling the seasonal dependence of the atmospheric response to observed El Niños in 1962–76. *Mon Weather Rev* 113:1970–1996
- Lau N-C, Lau K-M (1986) The structure and propagation of intraseasonal oscillations appearing in a GFDL GCM. *J Atmos Sci* 43:2023–2047
- Liebmann B, Hartmann DL (1984) An observational study of tropical-midlatitude interaction on intraseasonal time scales during winter. *J Atmos Sci* 41:3333–3350
- Liebmann B, Hendon HH (1990) Synoptic-scale disturbances near the equator. *J Atmos Sci* 47:1463–1479
- Livezey RE, Chen WY (1983) Statistical field significance and its determination by Monte Carlo techniques. *Mon Weather Rev* 111:46–59
- Manabe S, Hahn DG (1981) Simulation of atmospheric variability. *Mon Weather Rev* 109:2260–2286
- Palmen E, Newton CW (1969) *Atmospheric circulation systems*. Academic Press, Orlando, Florida
- Palmer TN (1982) Properties of the Eliassen-Palm flux for planetary motions. *J Atmos Sci* 39:992–997
- Randel WJ (1992) Upper tropospheric equatorial waves in ECMWF analyses. *Q J R Meteorol Soc* 118:365–394
- Randel WJ, Held IM (1991) Phase speed spectra of transient eddy fluxes and critical layer absorption. *J Atmos Sci* 48:688–697
- Randel WJ, Stanford JL (1985) An observational study of medium-scale wave dynamics in the Southern Hemisphere summer. Part I: wave structure and energetics. *J Atmos Sci* 42:1172–1188
- Wallace JM, Lau N-C (1985) On the role of barotropic energy conversions in the general circulation. *Adv Geophys* 28:33–74
- Warn T, Warn H (1978) The evolution of a non-linear Rossby wave critical level. *Studies Appl Math* 59:37–71
- Webster PJ (1973) Remote forcing of the time-independent tropical atmosphere. *Mon Weather Rev* 101:58–68
- Webster PJ, Holton JR (1982) Cross-equatorial response to middle-latitude forcing in a zonally varying basic state. *J Atmos Sci* 39:722–733
- Zhang C, Webster PJ (1992) Laterally forced equatorial perturbations in a linear model. Part I: stationary transient forcing. *J Atmos Sci* 49:585–607